Durability monitoring of reinforced concrete

Yurena Seguí Femenias[1], Ueli Angst[1], and Bernhard Elsener[1,2]

[1] ETH Zürich, Institute for Building Materials (IfB), Stefano-Franscini-Platz 3, 8093 Zurich, Switzerland
[2] University of Cagliari, Department of Chemical and Geological Sciences, 09100 Monserrato (CA), Italy

ABSTRACT: Corrosion is the main cause of failure in steel reinforced concrete structures. In a non-carbonated chloride-free concrete, the steel reinforcement stays passive; however, this passivity can be destroyed due to ingress of chloride ions or carbonation of the cement paste. In this work, Ag/AgCl ion-selective electrodes (Ag/AgCl ISE), used as chloride sensor, and thermally oxidized iridium electrodes (IrO_x), used as pH sensor, have been developed to be embedded in concrete. Both sensors were calibrated in solutions simulating the concrete environment and tested in mortar samples in the laboratory. The results obtained show that the studied electrodes can be successfully used to monitor chloride concentrations and changes in pH in the concrete pore solution.

1 INSTRODUCTION

Reinforced concrete is the most common building material used in public infrastructures and private buildings. In the alkaline concrete environment, reinforcing steel is protected from corrosion by a thin oxide film (passive film). The reinforcing steel can, however, be depassivated when the concrete carbonates (carbonation-induced corrosion) (Elsener et al., 2013) or when a certain concentration of chlorides reach the reinforcement (chloride-induced corrosion) (Elsener et al., 2013).

Concrete structures damaged by reinforcement corrosion have to be repaired in order to reach their expected service life. In order to apply protective and repair techniques in the most simple and cost-effective way, detection of corrosion risk and/or determination of the rate of deterioration are important (Gulikers, 2016). In fact, most of the current monitoring methods in concrete structures aim at measuring the relevant parameters regarding corrosion risk and propagation. For example, the so-called anode-ladder system is based on the measurement of a macrocell current (established between steel reinforcement and anode-ladder) and it allows monitoring the time to depassivation (Raupach et al., 1997, Raupach et al., 2001). There are also several sensors based on in-depth resistivity measurements, such as the so- called multi-ring electrode (Schiessl et al., 1995), that provide information on the corrosion risk. Other techniques are based on embedded reference electrodes. Their use permit obtaining electrochemical data (such as steel potential and linear polarization resistance), from which the time to depassivation and corrosion rate is calculated (Elsener et al., 2013).

In this work, Ag/AgCl ion-selective electrodes (Ag/AgCl ISE) and thermally oxidized iridium electrode IrO_x, to be used as chloride and pH sensors respectively, have been developed. Whereas the use of the Ag/AgCl ion-selective electrode (Ag/AgCl ISE) is a well-established method to measure the free chloride concentration in the concrete pore solution (Angst et al.,

2010, Jin et al., 2017, Seguí Femenias et al., 2015), a reliable pH sensor to be embedded in concrete still does not exist (Plusquellec et al., 2017).

These sensors are used for the non-destructive in-situ measurement (monitoring) of the two most relevant parameters for corrosion, i.e., the chloride concentration and pH of the pore solution. This would permit predicting the service life of the structure in a non-destructive and more accurate way.

2 THEORETICAL BACKGROUND

2.1 The silver/silver chloride ion-selective electrode

The silver/silver chloride ion-selective electrode (Ag/AgCl ISE) used in this work is a commercial electrode consisting of a silver wired covered by a layer of silver chloride. In presence of chlorides, the potential response of the Ag/AgCl ISE is (Koryta, 1972):

$$E_{Ag/AgCl\ ISE} = E^0_{Ag/AgCl\ ISE} - \frac{RT}{F}\ln a_{Cl^-} \tag{1}$$

where R is the gas constant, F the Faraday constant, T the absolute temperature, and $E^0_{Ag/AgCl\ ISE}$ is the electrode standard potential ($E^0_{Ag/AgCl}$ =225.6 mV vs. Ag/AgCl/sat. KCl at 20 °C (Shreir, 1994). The Ag/AgCl ISE potential also depends on temperature (Shreir, 1994) and other ions that may be dissolved in the test solution (Seguí Femenias et al., 2015). Regarding the interference of other ions, the Ag/AgCl ISEs have been shown to be feasible for monitoring of chloride concentrations in concrete structures, except in presence of sulfide ions (Seguí Femenias et al., 2015).

2.2 The iridium oxide electrode

Thermally oxidized iridium wires were produced based on the procedure reported in (Yao et al., 2001). The details of the production protocol are reported in the following work (Seguí Femenias et al., 2017). The most common accepted pH-sensing mechanism of thermally oxidized iridium is based on the transition between Ir (IV) to Ir (III), involving the participation of one proton H^+. The Nernst equation that dictates the potential of the IrO_x is written as (Pourbaix, 1974):

$$E_{IrO_x} = E^0_{IrO_x} - \frac{RT}{F}pH \tag{2}$$

Different electrode standard potentials $E^0_{IrO_x}$ and slopes for the E_{IrO_x}-pH response are obtained depending on the production method and exposure conditions (Kakooei et al., 2013, Olthuis et al., 1990, Trasatti, 1991). In this work, the IrO_x electrodes were immersed in alkaline solution (pH values between 9 and 13.5) for months to simulate the concrete environment. The iridium oxide pH-sensors (IrO_x electrodes) were then calibrated in pH values between 13.5 and 9.

2.3 Potential response of the electrodes

The electrodes used in this work (silver/silver chloride ISE and iridium oxide electrode IrO_x) were calibrated in solution before being embedded in concrete. Figure 1a shows experimental data on the potential $E_{Ag/AgCl\ ISE}$ of the Ag/AgCl ISE as a function of the logarithm of the chloride activity as reported in previous works (Seguí Femenias et al., 2015). Figure 1b shows

experimental data on the potential E_{IrO_x} of an iridium oxide electrode IrO_x as a function of the pH of the solution. The obtained values (from the linear fit) for the E_{IrO_x}-pH intercept ($E^0_{IrO_x}$) and for the E_{IrO_x}-pH slope are 0.723 V (vs. Ag/AgCl/sat. KCl) and -0.053 V/pH respectively.
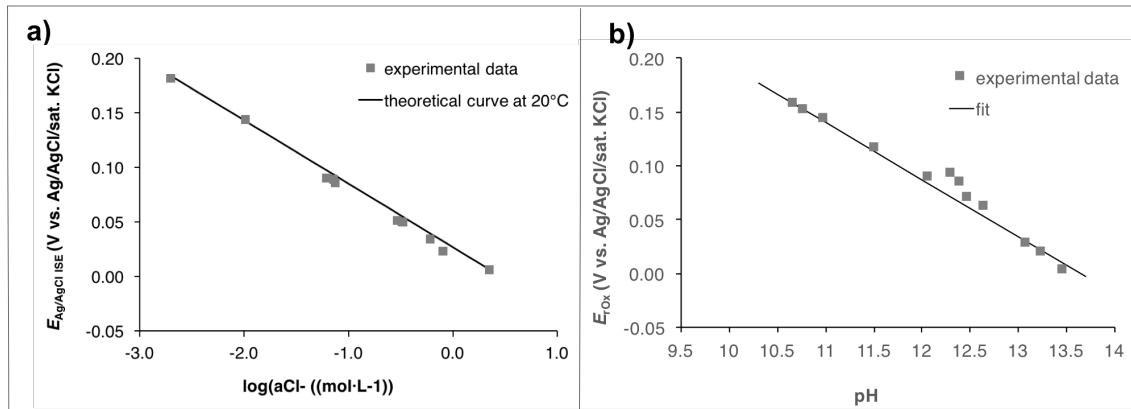

Figure 1. (a) Potential $E_{\text{Ag/AgCl ISE}}$ of the Ag/AgCl ISE as a function of the logarithm of the chloride activity, together with the theoretical curve at 20°C (Seguí Femenias et al., 2015) (b) Potential E_{IrO_x} of an IrO_x electrode (IrO_x 2, in Figure 3) as a function of the pH of the solution, together with the calculated linear fit.

3   METHODS

Two rectangular mortar prism were produced with embedded Ag/AgCl ISEs and IrO_x electrodes in each case. The mortar mix proportions were cement/water/sand 1: 0.5: 2 with CEM I 52.5, with sand size <1mm. For the first sample, three Ag/AgCl ISEs (ISE 1, ISE 2 and ISE 3 in Figure 2a) and three structural steel rods (steel 1, steel 2 and steel 3 in Figure 2a) were embedded. For the second sample, three IrO_x electrodes (IrO_x 1, IrO_x 2 and IrO_x 3 in Figure 2b) were embedded. In both cases, an internal reference electrode was also embedded (Figure 2a and 2b).

The samples were cured for one week at 95%RH and 21°C and then all the surfaces (with the exception of one surface, parallel to the embedded sensors) were painted with an epoxy-resin. The surface of the cube with embedded ISEs that was not coated was put in contact with synthetic pore solution (0.2 mol·L^{-1} KOH 0.15 mol·L^{-1} NaOH sat. Ca(OH)$_2$) containing 2 mol·L^{-1} NaCl, so one-dimensional chloride transport process occurred. The sample with the embedded IrO_xs was placed in a carbonation chamber (65%RH, 21°C and 4% CO$_2$) so one-dimensional carbonation occurred though the non-coated surface. The main features of the two set-ups are shown in Figure 2. In both cases, the mentioned sensors were embedded in the mortar at different cover depths, in order to monitor the penetration of the corrosive agent.

In both cases, a reference electrode was embedded in the mortar in order to be used as internal reference electrode (Figure 2a and 2b). The potential of the ISEs, steel rods (Figure 2a) and IrO_x electrodes (Figure 2b) was continuously measured versus this embedded reference electrode. In both cases, the potential of the internal reference was periodically measured (and corrected for the liquid junction potential (Angst et al., 2008)) with an external reference electrode that was

inserted in the upper opening ("hole for contact with external RE" in Figure 2a and 2b) on the sample surface.
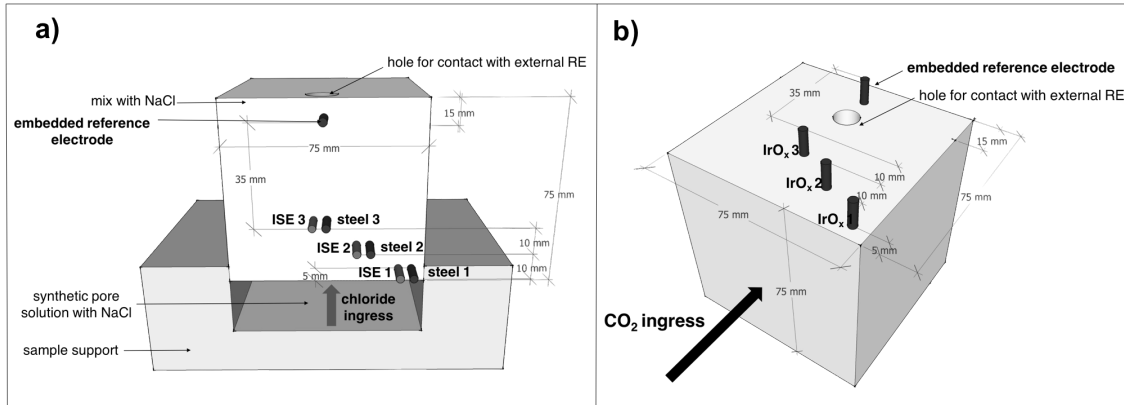

Figure 2. Main features of the set-up used to monitor (a) chloride ingress and corrosion state with embedded Ag/AgCl ISEs and steel rods respectively (b) carbonation propagation with embedded IrO_x electrodes. All the surfaces were coated with epoxy resin with the exception of the surface of chloride ingress (a) and CO_2 ingress (b).

All the experiments were carried out at room temperature (20-21 °C). After ca. 140 days, the experiment with embedded ISEs ended and slices of approximately 5mm-thick containing each embedded ISE/steel rod were cut and grinded. Approximately 20 g of mortar powder were taken from each slice and the total chloride content was determined by the acid digestion / potentiometric titration method. The experiment with embedded IrO_x electrodes was finished after ca. 170 days. The sample was then split in half (perpendicular to the surface of CO_2 ingress) and the carbonation front was determined by spraying thymolphthalein pH-indicator.

4   RESULTS AND DISCUSSION

4.1   Ag/AgCl ISEs embedded in concrete to monitor chloride ingress and corrosion state

Figure 3a shows the chloride concentration as a function of time for the Ag/AgCl ISE at each cover depth. Figure 3b shows the chloride concentration as a function of cover depth for some selected times (20, 60, 100, and 140 days). Figure 3c shows the chloride concentration (from the last potentiometric measurement performed) as a function of the total chloride content. Note that the for the calculation of the concentrations, the activity coefficients of chloride ions in cement paste were taken from (Vera et al., 2000).

From Figure 3a, the chloride concentration increased with time, especially during the first 60 days. The chloride concentration is markedly higher for the smaller cover depths. This can be clearly seen in Figure 3b.

Figure 3c shows the relation between the chloride concentration measured with the ISEs (free chlorides) and the results obtained from the total chloride content. The total chloride content includes both the free (dissolved in the pore solution) and the bound chlorides (i.e., those bound to the hydration products of the binder in concrete). In the present study, relatively high chloride concentrations were achieved within short exposure time, mostly due to the low cover depth. The high concentrations may explain the observed linearity in the relationship between free and

total chlorides. At low to moderate chloride concentrations, this relationship is well-known to be nonlinear (Luping et al., 1993).
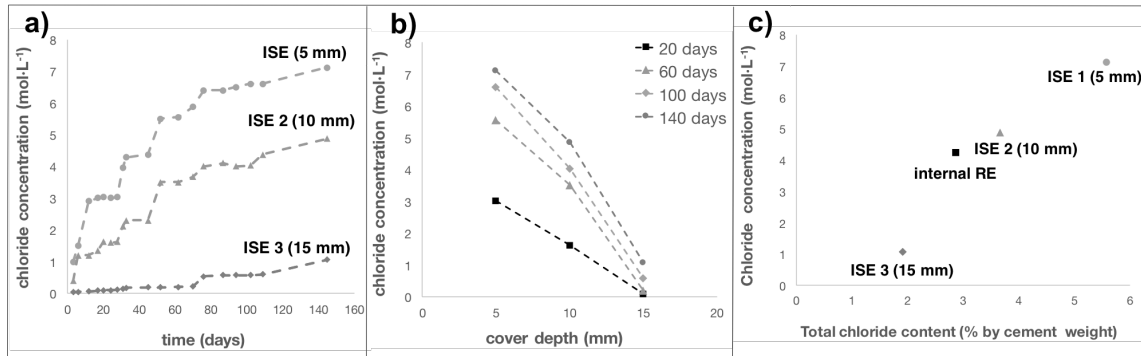

Figure 3. (a) Chloride concentration as a function of time for the Ag/AgCl ISE at each cover depth (5, 10 and 15 mm) (b) Chloride concentration as a function of cover depth for some selected times (20, 60, 100, and 140 days) (c) Chloride concentration (from the last potentiometric measurement performed) as a function of the total chloride content at each ISE location (Figure 2).

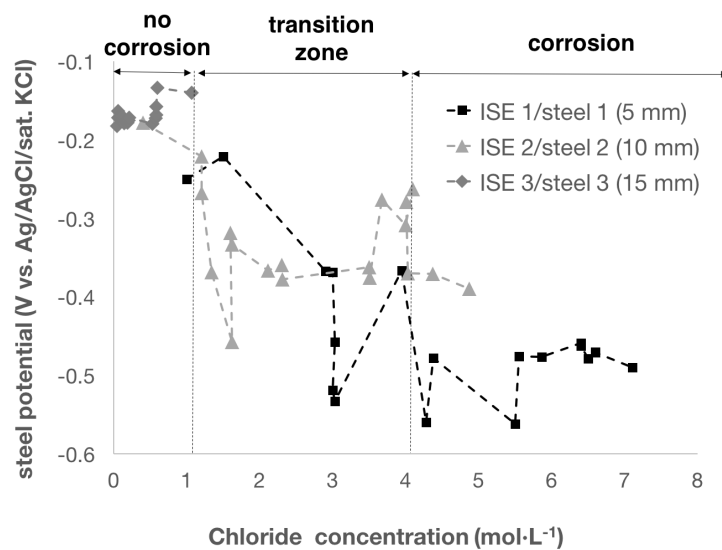Figure 4 shows the steel potential versus the chloride concentration at each cover depth.

Figure 4. Steel potential vs. chloride concentration at each cover depth (5, 10, and 15 mm). The zones defined in the graph (no corrosion, transition zone, corrosion) schematically represent the corrosion state of the steel (compare text).

From Figure 4, it can be seen that for chloride concentrations below 1 mol·L^{-1} (no corrosion), the steel potential was relatively constant; variations in potential were smaller than 50 mV. For chloride concentrations between 1 and 4 mol·L^{-1} (transition zone), the steel potential overall decreased but it occasionally increased. Transition from passive to active state is not immediate and it is believed that this behaviour was due to local depassivation and further repassivation. At

chloride concentrations above 4 mol·L^{-1} (corrosion zone) the steel potential had decreased at least 200 mV with respect to the initial value. Such potential differences are usually related to corrosion initiation (Elsener et al., 2013).

From the results presented in this test, it can be seen that the combined measurement of steel potential and chloride concentration provide reliable data for assessing the corrosion risk of the reinforcement.

4.2   *IrO$_x$ embedded in concrete to monitor carbonation propagation*

Figure 5 shows the potential of the IrO$_x$ electrode embedded at 15 mm cover depth (IrO$_x$ 2 in Figure 2b) and the pH as a function of exposure time in the carbonation chamber. The potential measured was corrected for the diffusion potential (Angst et al., 2008) established between IrO$_x$ and internal reference electrode due to the pH gradient. The pH was calculated from the calibration curve shown in Figure 1b.
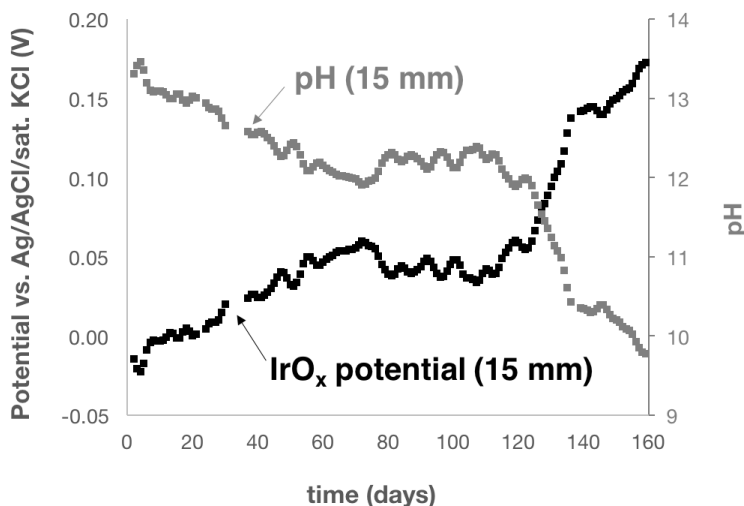

Figure 5. Potential of the IrO$_x$ electrode embedded at 15 mm cover depth (IrO$_x$ 2 in Figure 2b) and the calculated pH as a function of time of exposure in the carbonation chamber.

With this experimental approach, combining an embedded reference electrode and an embedded pH sensor, it was possible to follow for the first time the change of the pore solution pH in the mortar sample continuously and in-situ (directly in the carbonation chamber), showing interesting results on the carbonation process. The IrO$_x$ potential increased by 50 mV during the first 60 days, corresponding to a pH decrease from 13.4 to approximately 12.5 (Figure 5). For the following 60 days, the pH remained quite stable at 12.5. Then a rapid drop of pH was observed: after 160 days in the carbonation chamber, the pH decreased to ca. 10 (Figure 5).

The interpretation of these results is similar to a titration curve. The initial pH decrease down to ca. 12.5 was due to the consumption of the alkalinity from the KOH and NaOH in the pore solution. The constant pH registered afterwards is due to the gradual consumption of the alkaline reserve provided by Ca(OH)$_2$, calcium hydroxide being the hydration product providing the buffer capacity of the concrete pore solution (Glass et al., 2000). The marked pH decrease observed afterwards is probably due to the rapid consumption of the pore solution alkalinity in the absence of a buffer. The results from the thymolphthalein test, performed at the end of the

exposure testing showed a carbonation front of ca. 12-15 mm; thus, in agreement with the results of the sensors.

5   CONCLUSIONS AND OUTLOOK

The results obtained in this work show that the Ag/AgCl ISE and the IrO_x electrodes can be successfully used to monitor changes in chloride content and pH continuously and in-situ in the concrete pore solution of reinforced concrete. The sensors have shown to work reliably also at relative humidity of 65%. The possible applications are:

a) *Research*: the pH sensor can be applied to study the carbonation rate of new binders with lower clinker content. In contrast to the laborious traditional, destructive tests with phenolphthalein spraying on the concrete surface that give only a yes/no answer, with the in-situ sensors the carbonation process can be followed more in detail. It will be possible to relate the time at pH 12.5 (consumption of the $Ca(OH)_2$ buffer) to the amount of clinker in the cement.

b) *Condition monitoring and assessment*: knowing the pH and/or the chloride concentration at different depths in reinforced concrete over time will allow predicting further propagation of the CO_2 or chloride ingress into concrete. This would be especially useful to predict residual service life of structures exposed to high chloride concentrations (de-icing salts) or high CO_2 concentrations (road tunnels). Figure 6 shows two examples of how the sensors may be applied in engineering structures.
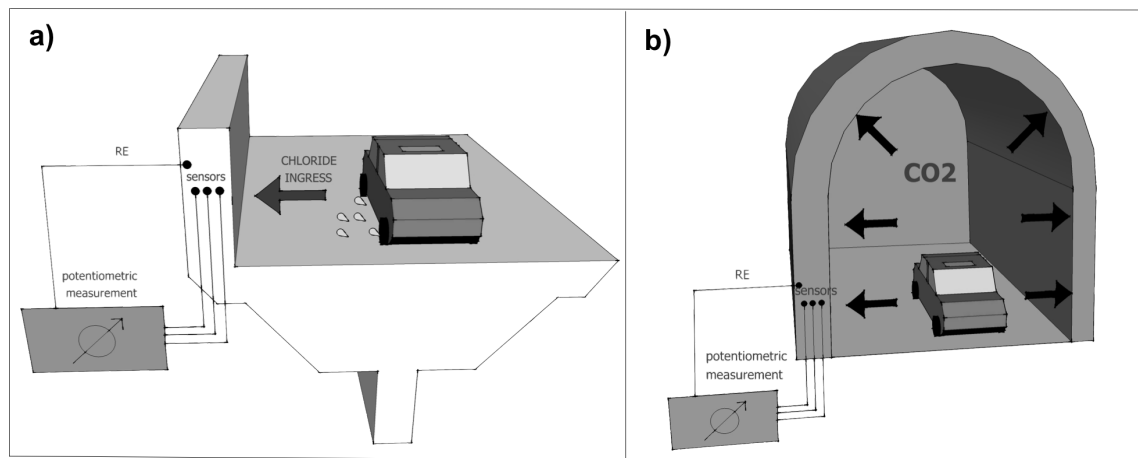

Figure 6. Schematic depiction of the set-up proposed to detect chloride ions and variations in pH in concrete structures exposed to (a) high chloride concentrations (e.g., as bridges exposed to deicing salts) (b) high CO_2 concentrations (e.g., tunnels).

6   REFERENCES

Angst, Elsener, Larsen and Vennesland, 2010, Potentiometric determination of the chloride ion activity in cement based materials, *J. Appl. Electrochem.,* 40**,** 561-573. doi: 10.1007/s10800-009-0029-6.

Angst, Vennesland and Myrdal, 2008, Diffusion potentials as source of error in electrochemical measurements in concrete, *Mater. Struct.,* 42**,** 365-375. doi: 10.1617/s11527-008-9387-5.

Elsener, Bertolini, Pedeferri and Polder, 2013, *Corrosion of steel in concrete, second ed.* Weinheim: Willey.

Gulikers, 2016, What are the benefits of corrosion monitoring in concrete structures from an owner's perspective?, *Concr. Solutions***, 19-24.

Jin, Jiang and Zhu, 2017, Monitoring chloride ion penetration in concrete with different mineral admixtures based on embedded chloride ion selective electrodes, *Constr. Build. Mater.,* 143**, 1-15. doi: 10.1016/j.conbuildmat.2017.03.131.

Kakooei, Ismail and Ari-Wahjoedi, 2013, An overview of pH sensors based on iridium oxide: fabrication and application, *Int. J. Mat. Sci Innovations,* 1**, 62-72.

Koryta, 1972, Theory and applications of ion-selective electrodes, *Anal. Chim. Acta,* 61**, 329–411. doi: 10.1016/S0003-2670(01)95071-8.

Luping and Nilsson, 1993, Chloride binding capacity and binding isotherms of OPC pastes and mortars, *Cem. Concr. Res.,* 23**, 247-253. doi: 10.1016/0008-8846(93)90089-R.

Olthuis, et al., 1990, pH sensor properties of electrochemically grown iridium oxide, *Sens. Actuators, B,* 2**, 247-256. doi: 10.1016/0925-4005(90)80150-X.

Plusquellec, et al., 2017, Determination of the pH and the free alkali metal content in the pore solution of concrete: Review and experimental comparison, *Cem. Concr. Res,* 96**, 13–26. doi: 10.1016/j.cemconres.2017.03.002.

Pourbaix, 1974, Atlas of electrochemical equilibria in aqueous solutions, *Pergamon Press,* 2nd ed.

Raupach and Schiessl, 1997, Monitoring system for the penetration of chlorides, carbonation and the corrosion risk for the reinforcement, *Constr. Build. Mater.,* 11**, 207-214. doi: 10.1016/S0950-0618(97)00039-1.

Raupach and Schießl, 2001, Macrocell sensor systems for monitoring of the corrosion risk of the reinforcement in concrete structures, *NDT&E Int.,* 34**, 435–442. doi: 10.1016/S0963-8695(01)00011-1.

Schiessl and Breit, 1995, Monitoring of the depth-dependent moisture content of concrete using multi-ring electrodes in *Concrete Under Severe Conditions: Environment and loading (Volume Two)*, United Kingdom.

Seguí Femenias, Angst, Caruso and Elsener, 2015, Ag/AgCl ion-selective electrodes in neutral and alkaline environments containing interfering ions, *Mater. Struct.* doi: 10.1617/s11527-015-0673-8.

Seguí Femenias, Angst and Elsener, 2017, Monitoring pH in corrosion engineering by means of thermally-produced iridium oxide electrodes, *(in preparation)*.

Shreir, 1994, *Corrosion control* IN *Corrosion,* third ed. Oxford: Butterworth-Heinemann Ltd.

Trasatti, 1991, Physical electrochemistry of ceramic oxides, *Electrochim. Acta,* 36**, 225-241. doi: 10.1016/0013-4686(91)85244-2.

Vera, et al., 2000, Chloride-ion activities in simplified synthetic concrete pore solutions: the effect of the accompanying ions, *J. Am. Ceram. Soc.,* 83 [3]**, 640-644. doi: 10.1111/j.1151-2916.2000.tb01245.x.

Yao, Wang and Madou, 2001, A pH electrode based on melt-oxidized iridium oxide, *J. Electrochem. Soc.,* 148**, H29-H36. doi: 10.1149/1.1353582.